Table.1 Features of Medicaid Personal care services male clients aged 65+ by Depressive symptoms

Full sample (M11Q) n=200	No Depressive symptoms n=179 (89.5%)	Depressive symptoms n=21 (10.5%)
Demographics		
Age, ±sd (yr)	78.92 ± 7.66	81.10 ± 7.38
Personal care services		
Hr/wk (mean±sd)	54.40 ± 44.45	61.76 ± 47.85
Duration (mean±sd)	7.60 ± 5.75	4.95 ± 3.29*
Medical status		
No of diseases (mean±sd)	5.01 ±1.35	5.58 ±1.63
Cognitive impairment		
No impairment, %	36.5	14.3
Dementia, %	63.5	85.7
Functional status		
No of ADL disabilities (mean±sd)	3.92 ± 1.66	4.33 ± 1.77
Sensory impairment		
Speech impairment, %	29.2	42.9
Visual impairment, %	44.9	66.7 *
Hearing impairment, %	43.3	76.2**
Muscular impairment		
Dominant hand/arm impairment, %	29.2	40.0
Upper extremities impairment, %	43.8	70.0*
Lower extremities impairment, %	71.8	80.0
Bladder incontinence, %	38.8	65.0 *
Socioenvironmental status		
Living situation		
Live Alone, %	59.3	44.4
Living with Caregiver, %	33.0	44.4
Living with Non-caregiver, %	7.7	11.1
Care-giving support		
No caregiver, %	14.3	22.2
Only live-in caregiver, %	22.0	33.3
Only out of home caregiver, %	52.7	33.3
Both in- and out- of home caregiver, %	11.0	11.1

*P<0.05 **P<0.01

Table2. Association between Variables and Depressive Symptoms: Multiple Logistic Regression

Dependent variable Frequency of Dependent Variable	Depressive symptoms (21/200) OR (95% CI), p
Personal care services	
Duration of services	0.86(0.75, 0.97)*, p=0.018
Functional status	
Sensory impairment	
Visual impairment	1.14 (0.38, 3.49), p=0.82
Hearing impairment	3.67 (1.18, 11.84)*, p=0.030
Muscular impairment	
Upper extremities impairment	2.61 (0.86, 7.65), p=0.082
Bladder incontinence	1.79 (0.63, 5.11), p=0.28

* P<0.05

Low testosterone level of middle-aged Japanese men—the association between low testosterone levels and the quality of life.

Mitsuko Yasuda M.D., M.P.H., Kumiko Furuya M.Sc., Takashi Yoshii M.D., Hisamitu Ide M.D., Satoru Muto M.D., Shigeo Horie M.D.

Department of Urology, Teikyo University School of Medicine

Key words: Salivary testosterone, Middle-aged Japanese men, The quality of life, Late- onset hypogonadism

To whom correspondence should be addressed:
Shigeo Horie M.D.
Department of Urology, Teikyo University School of Medicine
Address: 2-11-1 Kaga, Itabashi, Tokyo 173-8606 Japan
telephone number: +81-3-3964-2497
facsimile number: +81-3-3964-8934
shorie@med.teikyo-u.ac.jp

Abstract:

Background

Late-onset hypogonadism (LOH) is due to age-related steep declines in free testosterone levels in middle age. LOH can induce a variety of signs and symptoms which deteriorate the quality of life (QOL) of middle-aged men. The current study examined circadian rhythm of salivary testosterone levels in three cohorts: 20's-30's, 40's-50's, and 60's+ to investigate the association of QOL and testosterone level in Japanese adult men.

Subjects and Methods

Eighty-one healthy male Japanese volunteers and 20 LOH patients in their 40's- 50's were examined their salivary testosterone levels and independent variables including Body Mass Index (BMI), smoking rates, and SF36v2 as the health-related questionnaire to evaluate QOL. Saliva samples were collected at two-hour intervals between 9:00 am and 9:00 pm. Salivary testosterone levels were determined by Enzyme-Linked Immunosorbent Assay (ELISA, Demeditec Diagnostics, Germany).

Results

There were no significant differences in BMI and smoking rates among the three healthy groups. However, scores of SF36 related to body pain was significantly lower in 40's-50's than in 20's-30's. The mean salivary testosterone levels in 40's-50's were the lowest at any point of time except for 9:00 am among healthy cohorts and were similar to those of LOH patients.

A circadian rhythm was seen in salivary testosterone levels in the 20's-30's and 40's-50's groups, whereas it was lost in the 60's+ group and LOH patients.

Conclusion

Middle-aged Japanese men had the lowest levels of salivary testosterone and the worst quality of life related to body pain, which may affect their QOL.

Introduction:

The concept of age-related androgen deficiency in men, also termed late-onset hypogonadism (LOH) has opened up public awareness of the significance of men's health. Low testosterone levels affect physical, mental and sexual activities[2].

In contrast to women, men do not experience a sudden cessation of gonadal function comparable to menopause, although serum total testosterone gradually declines with advancing age, particularly after 50 years. Although serum testosterone levels are generally measured in the morning when they are at a peak, this circadian rhythm may be abolished or blunted in men with advancing age [3,4]. In healthy men, only 1-3% of biologically active steroids circulate freely with the balance bound tightly to sex hormone binding globulin (SHBG) or loosely to albumin. Free testosterone and the fraction bound loosely to albumin are readily available for entry into tissues. Unlike serum total testosterone, the concentration of SHBG significantly increases with age [4]. Consequently, serum free testosterone steeply decreases, which is considered to be associated with the incidence of LOH than with the decline of total serum testosterone [5,6]. Moreover, physical and psycho-social stress challenge homeostasis, increasing glucocorticoid secretion while decreasing testosterone levels [7].

In Teikyo Hospital, many patients who came to LOH outpatient services were white- collar workers in their 40's to 50's, half of whom suffered from depression[8]. Japan faces rapidly increasing suicide in middle-aged men mostly due to depression that may be associated with LOH. Previous studies of age-related testosterone decline have not focused on the testosterone levels in middle-aged men. We hypothesized that aside from aging, environmental stressors such as overwork escalate the steep decline of free testosterone levels, leading to the onset of LOH. We examined circadian rhythm of salivary testosterone levels in three cohorts: 20's-30's, 40's-50's and 60's+ to investigate the complexity of declining testosterone levels in later life. We used salivary testosterone as an alternative measure to evaluate serum free testosterone levels. Salivary testosterone is a useful, noninvasive and repeatable method of assessing levels of free testosterone because testosterone is not bound with protein in saliva [9].

Subjects and Methods:

Subjects

This study was approved by the institutional review board. Twenty-two healthy salaried men in a 20's-30's cohort (mean age: 30.32, range: 22-39), 32 in a 40's-50's cohort (mean age: 53.53, range:40-59) and 10 in a 60's+cohort were included in this study upon written consent. They were all white-collar workers in Tokyo. We also included 17 healthy retired men in their 60's to 70's. The healthy 60's+ cohort consisted of 27 men (mean age: 66.25, range: 60-74). We compared the healthy 40's-50's cohort with 20 new LOH patients in their 40-50's (mean age: 50.42, range 41-57) whose calculated free testosterone by the formula defined by International Society for the Study of the Aging Male (ISSAM) was lower than 72 pg/ml, the generally acceptable lower limits considered normal for testosterone substitution [10]. We

included both BMI and smoking habits that could affect testosterone levels. The subjects were asked about the history of smoking. If a subject quits smoking more than two years, he was counted as a non-smoker, as smoke-free two years can eliminate many adverse effects on health[11].

Health related-quality of life

The SF-36v2 was used to evaluate subject's health-related quality of life[12].

Saliva collection

Subjects were provided with plastic sterile screw sputum processors to collect samples at two-hourly intervals between 9 am and 9 pm. Subjects were asked to finish eating and brushing their teeth at least one hour before saliva sampling in order to avoid food and blood contamination. Subjects rinsed their mouths with water three times and waited a few minutes, then expectorated at least 1 ml of saliva directly into a collection vial. Testosterone levels in saliva increased post-micro-injury by brushing teeth [1].

It is noteworthy that testosterone levels remained elevated over the baseline well after micro-injury and even in samples that did not appear visually contaminated with blood. Importantly, the effect of microinjury was specific for testosterone. That is, after brushing neither salivary cortisol nor dehydroepiandrosterone levels were different than the baseline[13].

Sample storage

Salivary samples were stored up to three days at 4 °C in regular household refrigerators to avoid bacterial growth that could interfere with antibody binding and were then shipped cooled and stored at -20°C up to one month in laboratory freezers until analyzed.

Hormone determinations

A previous study proved that salivary concentration measured by a refined immunoassay was a reliable biomarker of serum free testosterone concentration [14,15]. Saliva testosterone levels were measured by ELISA (Demeditec Diagnostics, Germany). The efficacy of using ELISA was examined by the simultaneous measurements with Liquid Chromatography/Mass Spectrometry (LC/MS), which has high sensitivity and specificity.

Salivary testosterone measured by LC-MS and by ELISA showed a strong correlation ($r=0.84$), confirming the comparative validity with established kits of LC-MS for measuring salivary testosterone (Fig 1).

Statistics:

SPSS (15.0 version) was used for statistical analysis. As the data were normally distributed, One-Way ANOVA (post hoc t test) were used to compare the means of BMI, smoking rates and each dimension of quality of life on SF-36 among three healthy cohorts.

We performed post hoc t test in each of the 2-hour blocks to determine if there were any differences in hormone levels at a particular time of the day for each age group. In order to examine circadian rhythm, we analyzed data by repeated measures analysis of variance (ANOVA) for each of the 2-hour blocks in accordance with previous work that used a similar design [16-18] . Additionally, we used t-test to compare 40's-50's cohort with LOH patients.

Results:

First, we examined the circadian rhythm of testosterone levels in three healthy cohorts. Then we compared age-matched LOH patients with the healthy 40's-50's cohort to see whether

there were any similarities.

1) Healthy cohorts

The characteristics of subjects

The average age, BMI smoking rates, and health-related quality of life measured by SF-36v2 of each age group and p values by post hoc t test are shown in Table 1 and Table 2.

There were no statistically significant differences in either BMI or smoking rates among the three groups.

On the SF-36 v2, there was statistically worse quality of life related to body pain in the 40's-50's than in the 20's-30's cohort.

Salivary testosterone levels

A comparison of each age group at each 2-hour block is shown in Table 3.

Post hoc analysis showed that there were significantly lower testosterone levels in the 40's-50's cohort than in the 20's-30's cohort at all time points except for 7:00 pm. ($p=0.03$ for 9:00 am, $p<0.001$ for 11:00 am, $p=0.004$ for 1:00 pm, $p<0.001$ for 3:00 pm, $p=0.044$ for 5:00 pm, $p=0.070$ for 7:00 pm, $p=0.046$ for 9:00 pm). There were only two time blocks in which the testosterone levels were lower in the 60's+ than in the 20's-30's cohort ($p=0.007$ for 9:00 am, $p<0.001$ for 3:00 pm). There were no significant differences of mean testosterone levels at any time blocks between two older cohorts (40's-50's and 60's+).

Analysis of the circadian rhythm (Fig 2)

The repeated-measures ANOVA showed significant main effects of time in the cohort of 20's-30's ($p=0.047$) and 40's-50's($p=0.022$), confirming the circadian pattern. However, there was no main effect of time in the cohort of 60's+ ($p=0.404$), indicating the lack of circadian rhythm.

The pattern of circadian rhythm

The repeated-measures of ANOVA for the 20's-30's and 40's-50's cohorts showed significant group-by-time interaction ($p=0.002$). It suggested that two group had the different pattern of circadian rhythm.

2) Comparison of the healthy 40's-50's cohort with LOH patients (Fig 3)

There were significantly lower testosterone levels in LOH patients than in the healthy 40's-50's cohort at 11am ($p=0.016$), 7 pm (0.024) and 9 pm ($p=0.029$). In LOH patients, there was no circadian rhythm ($p=0.19$). Despite the similarity of testosterone levels, the scores for each domain of SF-36 v2 were significantly lower in LOH patients than in the 40's-50's cohort (Table 4).

In summary, the mean testosterone levels in the 40's -50's cohort were the lowest at almost every point of time among healthy cohorts and similar to those in LOH patients. A circadian rhythm of salivary testosterone levels was maintained in the 20s-30's and 40's-50's cohorts. However, their circadian patterns differed. The circadian rhythms were lost in the 60's+ and LOH patients.

Discussion

The healthcare community has paid much less attention to men's health than to woman's one so that the health care of men has tended to be piecemeal and somewhat uncoordinated[19].

In Japan, the average life expectancy was 78.6 years for men and 85.6 years for women in 2005[20]. Previous studies showed that steep decline of serum free testosterone contribute to the

onset of LOH [21,22].
Our preliminary study revealed two findings. 1) Testosterone levels of healthy middle-aged Japanese men were low, even though they maintained circadian rhythm; 2) Circadian rhythm was lost in the 60's+ cohort and LOH patients.
Testosterone secretion decline through both central (pituitary) and peripheral (testicular) mechanisms and its circadian rhythm becomes blunt or diminished [22]. Our study was consistent with the previous studies. In addition, our study showed that a progressive reduction in HPG function may occur in LOH patients as well as in aging men, which induce the loss of circadian rythmicity in saliva testosterone levels.
The decline of serum free testosterone is associated with aging as well as stressors, which challenge the homeostasis of endocrine environment. Stress and other conditions that elevate circulating adrenocorticotropine hormone (ACTH) and cortisol levels lead to depressed testosterone levels in animals and in men [24,25]. Excessive exposure to cortisol initiates apoptosis in rat Leidig cells, potentially contributing to suppression of testosterone levels[26]. Middle-aged men may be placed in a stressful environment and socio-environmental factors affect their mental health influencing physical health problems.

References:

1) Granger DA, Shirtcliff EA, Booth A, Kivlighan KT, Schwartz EB. The "trouble" with salivary testosterone. Psychoneuroendocrinolgy 2004; 29(10):1229-40.
2) Lunenfeld B, Saad F, Hoesl CE. ISM, ISSAM, and EAU recommendations for the investigation and monitoring of late-onset hypogonadism in males: scientific background and rationale. The Aging Male 2005; 8(2): 59-74.
3)Seidman SN. Testosterone Deficiency and Mood in Aging Men: Pathogenic and Therapeutic Interactions. World Biol Psychiatry 2003;4:14-20.
4) Seftel AD. Review: Male hypogonadism. Part I: Epidemiology of hypogonadism. International Journal of Impotence research 2006; 18:115-120.
5) Li JY, Li XY, Li M, Zhang GK, MA FL, Liu ZM, Zhang NY, Meng P. Decline of serum level of free testosterone on aging healthy Chinese men. The Aging Male 2005;8:203-204.
6) Iwamoto T, Yanase T, Koh E, Horie H, Baba K, Namiki M, Nawata H. Reference ranges of total serum and free testosterone in Japanese male adults. Nippon Hinyoukika Gakkai Zasshi. 2004; 95(6):751-60.
7) Dong Q, Salva A, Sottas CM, Niu E, Holmes M, Hardy MP. Rapid Glucocorticoid Mediation of Suppressed Testosterone Biosynthesis in Male Mice Subjected to Immobilization Stress. J Androl 2004; 25: 973-981.
8) Maruyama O, Ide H, Yoshi T, Nishio K, Saito K, Kurihara K, Okada H, Horie S. The Efficacy of 'Aging Male Questionnaire' (Kumamoto) for Japanese PADAM Patients. The Aging Male 2006;9:19.
9) Goncharov N, Gulinara K, Dobracheva A, Nizehnik A, Kolesnikova G, Herbst A, Westermann J. Diagnostic significance of free salivary testosterone measurement using a direct luminescence immunoassay in healthy men and in patients with disorders of androgenic status. The Aging Male 2006; 9(2):111-122.

10)Nieschlag E, Swerdloff R, Behre HM, Gooren LJ, Kaufman JM, Legros JJ. Lunenfeld B, Morley JE, Schulman C, Wang C., Weidner W, Wu FCW. Investigation, Treatment and Monitoring of Late-onset Hypogonadism in Males: ISA, ISSAM, and EAU Recommendations. European Urology 2005; 48: 1-4.
11) Brody LE. "How Cancer Rose to the Top of the Charts." *The New York Times*. February, 1, 2005.
12) McHorney CA, Ware JE Jr, Raczek AE. The MOS 36-item Short-Form Health Survey(SF-36):II. Psychometric and clinical tests of validity in measuring physical and mental health constructs. Med Care 1993;31: 247-63.
13) Kivlighan KT, Granger DA, Schwarts EB, Nelson V, Curran M, Shirtcliff EA. Quantifying blood leakage into the oral mucosa and its effects on the measurement of cortisol, dehydroepiandrosterone, and testosterone in saliva. Horm Behav 2004; 46(1):39-46.
14) Vittek J, L'Hommedieu DG, Gordon GG, Rappaport SC, Southren AL. Direct radioimmunoassay (RIA) of salivary testosterone: Correlation with free and total serum testosterone. Life Sci 1985; 37:711-6.
15) Villabona C. Salivary testosterone: relationship to total and free testosterone in serum. Clin Chem. 1986; 32: 231-2.
16) Di Giorgio A, Hudson M, Jerjes W, Clear AJ. 24-hour pituitary and Adrenal Hormone Profiles in Chronic Fatigue Syndrome. Psychosomatic Medicine 2005; 67(3): 433-440.
17) Jerjes WK, Cleare AL, Wessely S, Wood PJ, Taylor NF. Diurnal patterns of salivary cortisol and cortisone output in chronic fatigue syndrome. Journal of Affective disorders 2005; 87:299-304.
18) Abelson JL, Curtis GC. Hypothalamic-Pituitary-Adrenal Axis Activity in Panic Disorder. 24-hour secretion of Corticotropin and Cortisol. Arch Gen Psychiatry 1996; 53:323-331.
19) Duncan A, Hays T. The development of a men's health center at an integrate academic health center. The Journal of Men's Health & Gender 2005;2(1):17-20.
20) Ministry of Health, Labor and Welfare, Annual reports 2005.
21) Rhoden EL, Morgentaler A. Risk of testosterone-replacement therapy and recommendations for monitoring. N England J Med 2004; 350:482-492.
22) Harman DM, Metter EJ, Tobin JD, Peason J, Blackman MR. Longitudinal effects of aging on serum total and free testosterone levels in healthy men. Baltimore Longitudinal study of Aging. J Clin Endocrinol Metab 2001; 86:724-731.
23) Bremner WJ, Vitiello MV, Prinz PN. Loss of circadian rhythmicity in blood testosterone levels with aging in normal men. J Clin Endocrinol Metab 1983; 56:1278-1281.
24) Gao HB, Shan LX, Monder C, Handy MP. Supression of endogenous corticosterone levels in vivo increases the steroidogeneic capacityof purified rat Leidig cellsin vitro. Endocrinology 1996; 137(5): 1714-1718.
25) Roy M, Kirschbaum C, Steptoe A. Intraindivisual variation in Recent Stress Exposure as a Moderator of Cortisol and Testosterone levels. Ann Behav Med 2003; 26(3): 194-200.
26)Gao HB, Tong MH, Hu YQ, Guo QS, Ge R, Hardy MP. Glucocolticoid induces apoptosis in rat Leidig cells. Endocrinology. 2002; 143(1):130-138.

Table 1. Baseline characteristic of the healthy subjects

	Age, ± sd(yr)	BMI, ± sd	P value	Smoking rates(%)	P value
20′-30′ (n=22)	30.32 ± 4.45	22.73 ± 2.46	0.47	0.53 ± 0.51	0.99
40′-50′ (n=32)	53.53 ± 5.47	23.62 ± 2.37	0.83	0.52 ± 0.51	0.19
60+ (n=27)	66.25 ± 4.88	23.20 ± 1.98	0.83	0.21 ± 0.43	0.16

Table 2. Health-related quality of life on SF 36 v2 in healthy subjects

	Physical function	Role-physical	Body-pain	P value	General Health	Vitality	Social function	Role-emotional	Mental Health
20′-30′	57.38 ± 2.37	55.32 ± 2.21	58.45 ± 4.31*	*0.025	52.48 ± 8.21	51.36 ± 9.05	54.11 ± 5.39	52.31 ± 6.01	52.0 ± 6.67
40′-50′	54.84 ± 2.79	55.11 ± 3.03	51.13 ± 7.39*		52.54 ± 10.07	55.88 ± 6.40	51.62 ± 8.33	54.97 ± 2.19	53.32 ± 7.56
60+	54.88 ± 2.92	55.03 ± 3.69	54.98 ± 6.75		52.21 ± 6.54	56.18 ± 7.18	52.46 ± 6.54	53.53 ± 4.23	53.10 ± 7.71

Mean±sd *P=0.025

Table 3. Comparison of testosterone levels at each 2 hour block of time

	9am	P value	11 am	P value	1pm	P value	3pm	P value
20′-30′	66.82 ± 32.49	* 0.03	63.17 ± 23.59	*** <0.001	55.25 ± 10.60	** 0.004	61.47 ± 24.77	*** <0.001
40′-50′	47.33 ± 20.35	** 0.007	36.89 ± 7.30	0.135	37.60 ± 15.40	0.126	29.16 ± 13.22	*** <0.001
60+	41.17 ± 26.18	0.704	50.77 ± 28.11	0.075	44.54 ± 21.98	0.348	35.54 ± 13.47	0.414

	5pm	P value	7pm	P value	9pm	P value
20′-30′	51.58 ± 25.89	* 0.044	45.51 ± 19.06	0.070	45.72 ± 18.87	* 0.046
40′-50′	36.64 ± 12.87	0.232	32.81 ± 13.38	0.490	32.50 ± 13.57	0.230
60+	41.04 ± 24.33	0.741	38.54 ± 20.21	0.524	36.72 ± 20.82	0.696

*P<0.05, ** P<0.01, *** P<0.001

Table 4. The Scores of SF 36 v2
in 40's-50's cohort and LOH patients

	Physical function	Role-physical	Body-pain	General Health	Vitality	Social function	Role-emotional	Mental Health
40'-50'	54.84 ± 2.79	55.11 ± 3.03	51.13 ± 7.39	52.54 ± 10.07	55.88 ± 6.40	51.62 ± 8.33	54.97 ± 2.19	53.32 ± 7.56
LOH	45.25 * ± 7.56	37.77 ** ± 10.63	40.55 ** ± 7.24	35.42 ** ± 4.38	35.12 ** ± 7.92	32.43 ** ± 11.94	32.83 ** ± 16.26	39.37 ** ± 6.83

Mean±sd *p<0.01, **p<0.001

Fig 1. Correlation of Salivary testosterone levels measured by LC-MS with those by ELISA

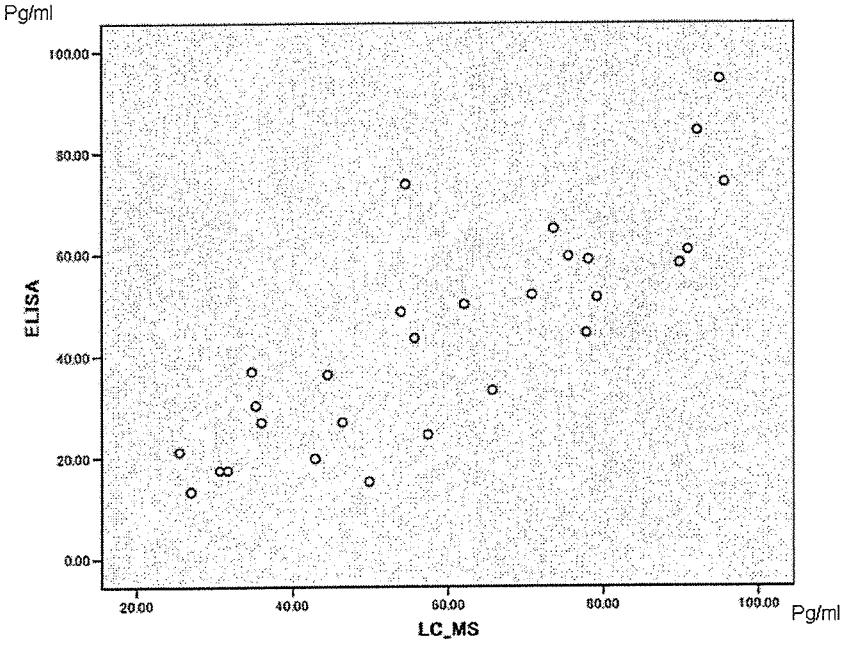

r=0.838
p<0.001

Fig 2. Circadian variations of salivary testosterone among healthy cohorts

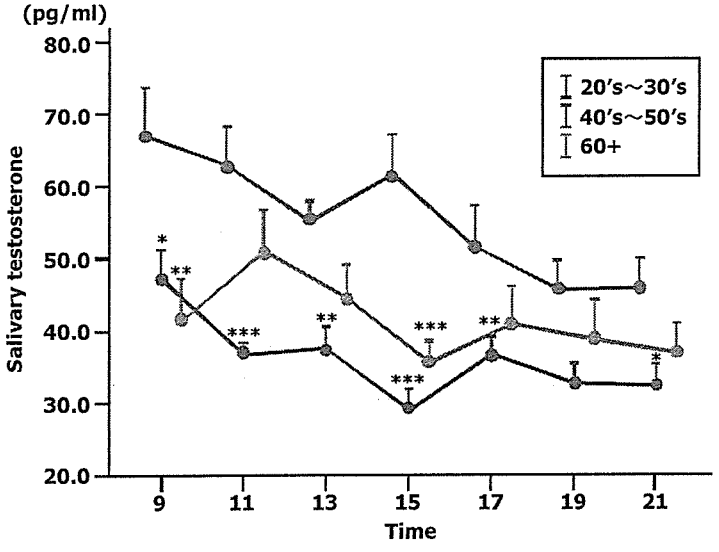

Fig 3.The comparison of healthy middle-aged men and LOH patients

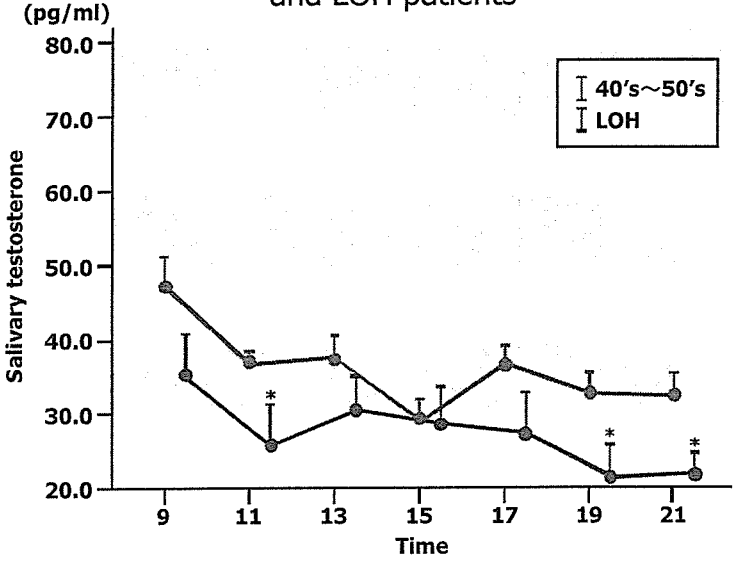

Available online at www.sciencedirect.com
SCIENCE DIRECT®
Biochemical and Biophysical Research Communications 341 (2006) 192–201
BBRC
www.elsevier.com/locate/ybbrc

Identification of the functional domains of ANT-1, a novel coactivator of the androgen receptor ☆

Shuli Fan, Kiminobu Goto [1], Guangchun Chen, Hidetaka Morinaga, Masatoshi Nomura, Taijiro Okabe, Hajime Nawata, Toshihiko Yanase *

Department of Medicine and Bioregulatory Science (3rd Department of Internal Medicine), Graduate School of Medical Sciences, Kyushu University, Maidashi 3-1-1, Higashi-ku, Fukuoka 812-8582, Japan

Received 29 November 2005
Available online 9 January 2006

Abstract

Previously, we identified a transcriptional coactivator for the activation function-1 (AF-1) domain of the human androgen receptor (AR) and designated it androgen receptor N-terminal domain transactivating protein-1 (ANT-1). This coactivator, which contains multiple tetratricopeptide repeat (TPR) motifs from amino acid (aa) 294, is identical to a component of U5 small nuclear ribonucleoprotein particles and binds specifically to the AR or glucocorticoid receptor. Here, we identified four distinct functional domains. The AR-AF-1-binding domain, which bound to either aa 180–360 or 360–532 in AR-AF-1, clearly overlapped with TAU-1 and TAU-5. This domain and the subnuclear speckle formation domain in ANT-1 were assigned within the TPR motifs, while the transactivating and nuclear localization signal domains resided within the N-terminal sequence. The existence of these functional domains may further support the idea that ANT-1 can function as an AR-AF-1-specific coactivator while mediating a transcription-splicing coupling.

Keywords: Androgen receptor; Activation function-1; Nuclear localization signal; Small nuclear ribonucleoprotein particle; Splicing factor compartment; Tetratricopeptide repeat; Transcriptional coactivator

The androgen receptor (AR) harbors two transcription activation function (AF) domains: the constitutively active AF-1 located in the N-terminal transactivating domain and the ligand-dependent AF-2 within the C-terminal ligand-binding domain [1]. The AR is considered to be quite unique among the members of the nuclear receptor superfamily, because most, if not all, of its activities are mediated via the ligand-independent constitutive activity of AF-1 [2,3]. This is in strong contrast to estrogen receptor α (ER α), in which the overall transactivation capacities are primarily dependent on AF-2 [4]. The AR shares hormone response element sequences on the DNA with the receptors for glucocorticoids (GR), mineralocorticoids, and progesterone [5]. In this regard, the N-terminal domain (NTD), which varies among these receptors, is thought to be responsible for the cell- and ligand-specific regulation of their target genes [6]. The fundamental role of AR-AF-1 was further supported by our clinical finding that the absence of an AR-AF-1-specific transcription coactivator results in androgen insensitivity syndrome [7]. To date, in addition to p300/CBP, SRC-1 and caveolin-1, which interact with both AF-1 and AF-2 [2,8,9], almost 20 proteins have been proposed to bind to the AR N-terminal transactivating domain, including basal transcription factors such as TFIIF [10], co-repressors [11–13], and

☆ *Abbreviations:* aa, amino acid(s); AF, activation function; ANT-1, androgen receptor N-terminal domain-binding protein-1; AR, androgen receptor; DHT, dihydrotestosterone; ER, estrogen receptor; GR, glucocorticoid receptor; NLS, nuclear localization signal; NTD, N-terminal domain; SFC, splicing factor compartment; snRNP, small nuclear ribonucleoprotein particle; TPR, tetratricopeptide repeat.

* Corresponding author. Fax: +81 92 642 5297.
E-mail address: yanase@intmed3.med.kyushu-u.ac.jp (T. Yanase).
[1] Present address: Internal Medicine and the Elderly Care, Kasamatsu-kai Medical Corporation Ariyoshi Hospital, Oo-aza Kamiariki 397-1, Miyata, Kurate-gun County, Fukuoka 823-0015, Japan.

0006-291X/$ - see front matter © 2005 Elsevier Inc. All rights reserved.
doi:10.1016/j.bbrc.2005.12.167

coactivators [14,15] as well as other unique proteins, including cyclin E [16], breast cancer susceptibility gene 1 (*BRCA1*) [17], and the RNA molecule SRA [18].

We previously isolated a cDNA sequence encoding a novel coactivator for the AR [19]. This protein, designated AR NTD transactivating protein-1 (ANT-1), bound to the AF-1 of the AR and GR, but not that of ER α, and specifically enhanced the AR- and GR-AF-1 transactivation capacities in a ligand-independent manner. The amino acid sequence of ANT-1 was identical to that of the PRP6 protein [20,21], a mammalian homolog of yeast prp6p, which forms U5 small nuclear ribonucleoprotein particles (snRNPs) involved in the spliceosome. In addition to ANT-1, cyclin E [22] and $p54^{nrb}$ [23], another AR-AF-1-binding protein, are also known to interact with splicing factors, suggesting that AR-AF-1 may be involved in the pre-mRNA splicing machinery. Upon confocal microscopic image analysis, ANT-1 was compartmentalized into 20–40 coarse splicing factor compartment (SFC) speckles against a background of diffuse reticular distribution [19]. Interestingly, the ANT-1 sequence shows structural significance, since it contains 19 copies of the tetratricopeptide repeat (TPR) motif, which plays significant roles in protein–protein interactions [24], in the final two-thirds of the C-terminal region.

It has been hypothesized that active gene transcription may occur simultaneously with pre-mRNA processing, and this process has been designated co-transcriptional splicing or "transcription-splicing coupling" [25,26]. Furthermore, steroid hormones affect the processing of pre-mRNA synthesized from steroid-sensitive promoters, but not from steroid-unresponsive promoters [27]. The nucleus contains different sets of functional compartments, often called "speckles," which include SFCs showing nearly 20–50 large speckles [28]. After three-dimensional reconstruction of confocal microscopic images, we observed that the activated AR forms 200–400 fine speckles that chiefly recruit AF-2-interacting transcriptional cofactors [29,30]. These speckles are mostly located in euchromatin regions and merge with the diffuse distribution of ANT-1. In contrast to cytoplasmic compartments, the subnuclear compartments are not sequestered by membrane structures, thereby allowing rapid movement of the protein components across the compartment. Therefore, interaction of ANT-1 with the AR or GR in the diffuse distribution of ANT-1 may play a role in the interaction between these two distinct subnuclear compartments. We speculated that it should contain at least four functional domains, namely a nuclear localization signal (NLS) domain, a transactivating domain, a speckle formation domain, and an AR-AF-1-binding domain. Therefore, in the present study, we performed analyses to investigate the presence of these functional domains in ANT-1.

Materials and methods

Cell culture. COS-7 cells and NIH3T3 fibroblast cells were maintained in Dulbecco's modified Eagle's medium supplemented with 10% fetal calf serum. To establish cells (designated COS-AR-AF-1 cells) that stably expressed AR-AF-1 (amino acids (aa) 1–532), COS-7 cells in 10 cm dishes were transfected with 5 μg of an AR-AF-1 expression plasmid [7] using the Superfect Transfection Reagent (Qiagen) according to the manufacturer's instructions. An initial selection was performed with 1 μg/ml of puromycin (Sigma) at 24 h after the transfection, and the selected cells were subsequently grown in bulk culture for 5–6 days. A single clone was isolated by limited dilution and then cultured for a further 2 weeks. The presence of the AR-AF-1 fragment in the stably transfected line was monitored by Western blotting using an anti-AR N-20 antibody (Santa Cruz Biotechnology).

Plasmids and site-directed mutagenesis. pMMTV-luc, containing the luciferase gene driven by the mouse mammary tumor virus long terminal repeat harboring a hormone response element for both the AR and GR, and the plasmids expressing ANT-N and ANT-C were described previously [7,19]. The expression plasmid for human ER α (pSG5-ER α) and a reporter plasmid for ER α (pERE2-tk109-luc) were provided by Dr. Shigeaki Kato (University of Tokyo, Tokyo, Japan). pANT-1-myc expressing myc-tagged full-length ANT-1 was prepared as described previously [19], and plasmids expressing truncated mutants of myc-tagged ANT-1 were obtained by appropriate restriction enzyme digestion or PCR amplification. Briefly, ΔANT(290) was obtained by restriction digestion with *Kpn*I and *Eco*RV. For ΔANT(146), ΔANT(172), ΔANT(399), ΔANT(499), and ΔANT(173–499) PCR was initially performed to create DNA fragments that contained a *Kpn*I restriction site at the 5′ end and an *Xba*I restriction site at the 3′ end. These fragments were then digested with *Kpn*I and *Xba*I, and subcloned into appropriate expression plasmids such as pcDNA3, pcDNA3-myc-his or pEGFP.

We used the Check Mate Mammalian Two-Hybrid System (Promega), in which the GAL-4 DNA-binding domain is present in a pBind plasmid, the herpes simplex virus VP16 activation domain is present in a pACT plasmid, and five GAL-4-binding sequences and a luciferase gene are present in the pG5luc plasmid. Truncated fragments of ANT-1 with an *Xba*I restriction site at the 5′ end and a *Kpn*I site at the 3′ end were obtained by PCR amplification and then subcloned into pACT to generate VP-ΔANT(146), VP-ΔANT(172), VP-ΔANT(290), VP-ΔANT(399), VP-ΔANT(499), and VP-ANT-C. Truncated fragments of the AR-NTD with a *Bam*HI restriction site at the 5′ end and an *Xba*I site at the 3′ end were also obtained by PCR amplification and then subcloned into pBind plasmids to generate GAL-AR(1–180), GAL-AR(180–360), GAL-AR(360–520), and GAL-AR(1–660).

Site-directed mutagenesis was performed using a Quick Change Site-directed Mutagenesis Kit (Stratagene) according to the manufacturer's protocols. The pEGFP plasmid harboring the ΔANT(172) sequence was used as a template.

Transient transfection and mammalian two-hybrid assays. COS-7 cells (5×10^5 cells per well in six-well plates) were transiently transfected using a Superfect Transfection Kit (Qiagen). Generally, 2.5 μg of plasmid DNA per well (0.2–1.0 μg of pcDNA3-ANT-1-deletion mutants, 0.2 μg of pCMVhAR [7], and 1.0 μg of pMMTV-luc) was used for the transfection, and the total amount of transfected DNA was kept constant by adding the pcDNA3 plasmid. At 16 h post-transfection, the cells were rinsed in PBS and then cultured in medium containing 10% charcoal-stripped fetal calf serum with or without a steroid hormone (10^{-8} M dihydrotestosterone (DHT)) for an additional 18 h. Subsequently, the cells were harvested and assayed for their luciferase activities using the Dual-Luciferase Reporter Assay System (Promega).

For mammalian two-hybrid assays, NIH3T3 cells were used according to the recommendations included in the Check Mate Mammalian Two-Hybrid System. At 24 h after plating at 10^5 cells per well in 12-well plates, the cells were transiently transfected with 500 ng of pG5luc, 100 ng of VP16 plasmids, and 300 ng of GAL4 plasmids. At 24 h post-transfection, luciferase assays were performed as described above.

Immunoprecipitation. Either COS-AR-AF-1 or COS-7 cells were subjected to transient transfection. Immunoprecipitation was performed as previously described [19]. Briefly, at 24 h post-transfection, whole cell lysates were prepared by lysing the cells in lysis buffer (1.0% Nonidet P-40, 50 mM Tris–HCl, pH 7.8, 150 mM NaCl, 1 mM DTT, and 1 tablet of

protease inhibitor mixture/10 ml buffer). After pre-clearing with protein G–Sepharose beads (Pharmacia), the lysates were incubated with an antibody against c-myc (Santa Cruz Biotechnology) for truncated ANT-1 or an antibody against the NTD of AR N-20 for the truncated ARs in immunoprecipitation (IP) buffer (1.0% Nonidet P-40, 50 mM Tris–HCl, pH 7.8, 200 mM NaCl, 1 mM DTT, and 1 tablet of protease inhibitor mixture/10 ml buffer) at 4 °C for 1 h, and then further incubated with protein G–Sepharose beads at 4 °C for 2 h. The immunoprecipitates were subsequently analyzed by Western blotting using antibodies against AR N-20 or c-myc.

Microscopy and imaging analysis. The cells were divided into 35-mm glass-bottomed dishes (MatTek Corporation) and then transfected with 0.5 μg of the plasmids using 2.5 μl Superfect reagent/dish. At 6–18 h post-transfection, the culture medium was replaced with fresh DMEM. The cells were first imaged without any hormone treatment and then incubated with 10^{-8} M DHT for 1 h. After the incubation, the cells were imaged again using a confocal laser scanning microscope (Leica TCS-SP system; Leica Microsystems). The green fluorescence in the cells was excited using the 488 nm line from an argon laser and the emission was viewed through a 500–550 nm band pass filter.

Results

Activation function and subcellular localizations of ANT-1 deletion mutants

In a previous paper, we demonstrated that an ANT-1 deletion mutant comprised of aa 78–495 (designated ANT-N) showed nearly full enhancement (about 90%) of the ligand-independent AR-AF-1 transactivation capacity of full-length ANT-1, while a deletion mutant comprised of aa 496 to the C-terminus of ANT-1 (designated ANT-C) did not show any enhancement [19]. Therefore, in the present study, ΔANT(499) covering the N-terminal half of ANT-1 was serially deleted from the C-terminal end to generate ΔANT(399), ΔANT(290), ΔANT(172), and ΔANT(146), respectively, in addition to ΔANT(173–499) (Fig. 1A). These fragments were then subcloned into appropriate plasmids to generate plasmids expressing the ANT-1 deletion mutants with and without fusion to GFP. As previously shown, full-length ANT-1 enhanced the transactivation function of the AR, which is activated in the presence of 10^{-8} M DHT, by inducing nearly four-fold enhancement of the AF-1 function. ΔANT(499), ΔANT(399), ΔANT(290), and ΔANT(172) each enhanced the AR-dependent transactivation by about 90% of the level induced by full-length ANT-1, indicating that aa 78–172 are important for the transactivation induced by ANT-1 (Fig. 1B). In contrast, when aa 147–172 were deleted (ΔANT(146)), the transactivation function was almost negligible. This result was further confirmed by the findings that neither ΔANT(173–499) nor ANT-C were able to induce any transactivation.

Next, we investigated the subcellular and intranuclear distributions of the ANT-1 deletion mutants fused in-frame to GFP. Representative confocal microscopic images of COS-7 cells transfected with the expression plasmids for the fusion proteins are shown in Fig. 2. As previously demonstrated, full-length ANT-1-GFP showed two distinct distributions in the nucleus: a diffuse reticular distribution

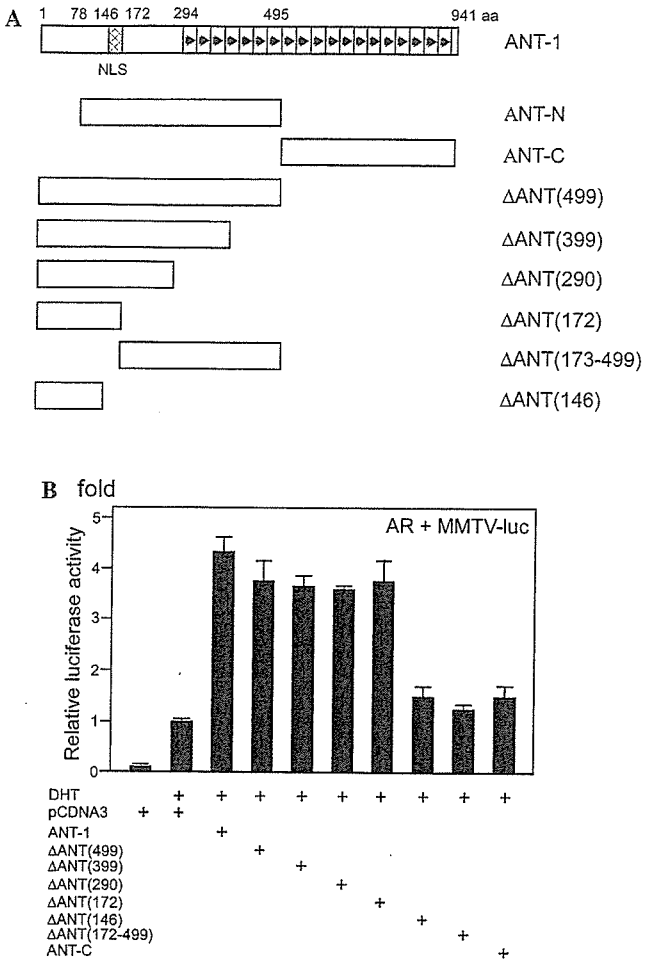

Fig. 1. Schematic diagrams of the human ANT-1 deletion mutants and their transactivation functions. (A) Schematic diagrams of the ANT-1 truncated mutants used in the experiments. The structure of full-length ANT-1 is shown at the top. ANT-1, a binding protein for U5 snRNP, consists of 941 aa and possesses 19 TPR motifs from aa 294 within the last two-thirds of the C-terminal region (shown by arrowheads in open boxes). The putative NLS is shown as a hatched box. ANT-N (aa 78–495) and ANT-C (aa 495–941) were reported previously. All the truncated fragments were subcloned into appropriate plasmids and subjected to reporter assays, confocal microscopic observation, mammalian two-hybrid assays, and immunoprecipitation. (B) Transactivation functions of the truncated mutants of ANT-1. COS-7 cells were transfected with the empty pcDNA3 plasmid (pcDNA3) or pcDNA3 harboring full-length ANT-1 or its deletion mutants (ΔANT(499) to ANT-C), a plasmid expressing the full-length AR (molar ratio 5:1) and a pMMTV-luc reporter plasmid, and then treated with 10^{-8} M DHT. The relative enhancement of the luciferase activity compared with that after co-transfection with the empty pcDNA3 plasmid in the presence of 10^{-8} M DHT is expressed as the -fold induction.

throughout the nucleus and 20–40 coarse subnuclear speckles (Fig. 2A) [19]. ΔANT(499)-GFP and ΔANT(399)-GFP showed similar distributions in the nucleus to the full-length fusion protein (Figs. 2B and C). In contrast, ΔANT(290)-GFP, which lacked aa 290–399, did not form any subnuclear speckles and showed only a diffuse distribution in the nucleus (compare Figs. 2C and D), while retaining the transactivation function on the AR (Fig. 1B). These results suggest that the region required for ANT-1 to

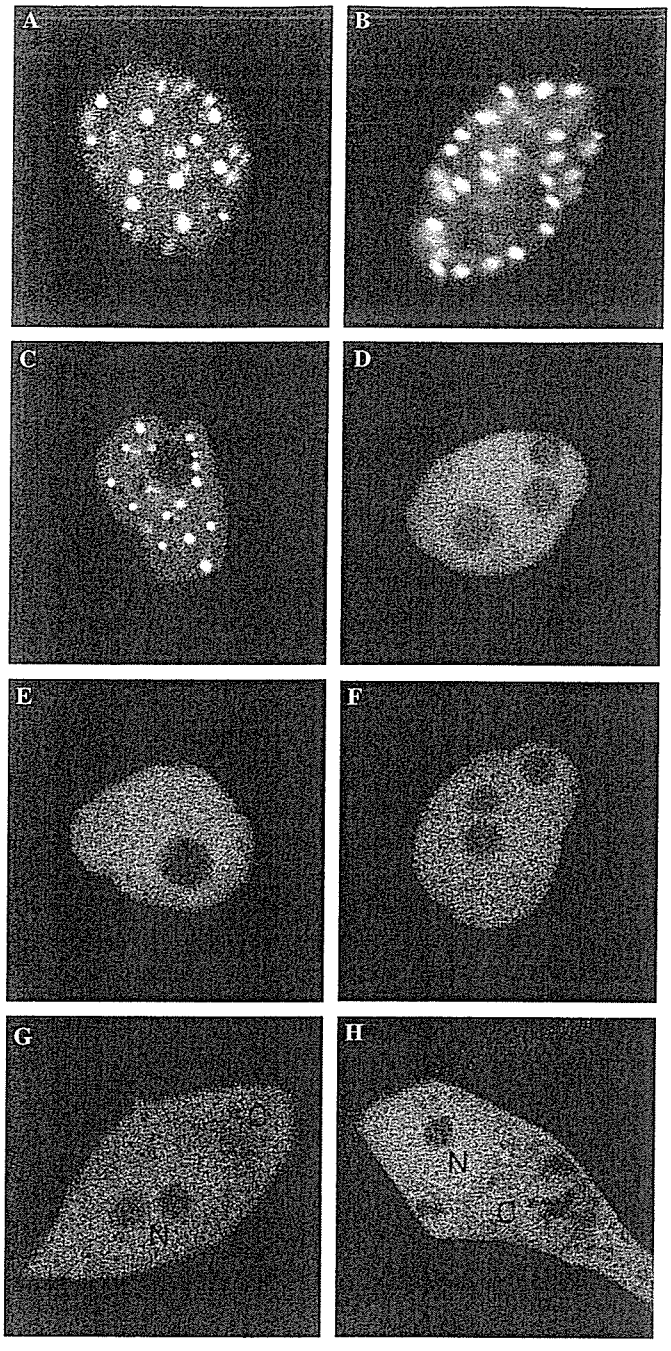

Fig. 2. Confocal microscopic images of the full-length and truncated mutants of ANT-1 fused to GFP. (A–H) COS-7 cells were transiently transfected with pEGFP harboring full-length ANT-1 (A) or its truncated mutants (B–H) and then observed by confocal microscopy. (B) ΔANT(499); (C) ΔANT(399); (D) ΔANT(290); (E) ΔANT(200); (F) ΔANT(172); (G) ΔANT(146); (H) ΔANT(173–499). In addition to the ANT-1 deletion mutants shown in Fig. 1A, a deletion mutant of ANT-1 comprising aa 1–200 (E) was used in the experiments. In (A–F) only the nucleus shows fluorescence. In (G,H) N, nucleus; C, cytoplasm.

generate intranuclear speckles is located between aa 291 and 399, and that speckle formation is not required for the transactivation function of ANT-1. Furthermore, ΔANT(146)-GFP and ΔANT(173–499)-GFP were not concentrated in the nucleus, but diffusely distributed throughout both the nucleus and the cytoplasm, suggesting that the 26 aa sequence from aa 146 to 172 confers nuclear localization (compare Figs. 2F and G).

The NLS and receptor-specific transactivation capacity of ANT-1

The region from aa 145 to 172 contains bipartite basic amino acid stretches, often found in an NLS, separated by a 20 aa interval, namely Lys(146)-Arg(147)-Lys(148) and Lys(169)-Arg(170)-Arg(172). Thus, using the plasmid expressing ΔANT(172)-GFP as a template, we performed site-directed mutagenesis to mutate these basic amino acids in the first stretch alone (ΔANT(172)M1), the second stretch alone (ΔANT(172)M2 and M3), and both stretches (ANT(172)M4 and M5) (Fig. 3A). The mutated plasmids were then transfected into COS-7 cells and observed by confocal microscopy (Fig. 3B). ΔANT(172)M1, ΔANT(172)M2, and ΔANT(172)M3 all showed partial disruption of the nuclear concentration of the fluorescence (panels b–d), thereby generating cytoplasmic fluorescence. When both the first and second stretches were simultaneously mutated, the nuclear translocation of the fusion proteins (ΔANT(172)M4 and ΔANT(172)M5) was almost completely disrupted and resembled that of ΔANT(146) (panels e and f), indicating that these bipartite basic amino acid stretches are the NLS of ANT-1.

When the transactivation capacities of these ΔANT(172) mutants were compared with that of wild-type ΔANT(172), we found that the transactivation function of each mutated fragment was almost completely abolished. As shown in Fig. 3C, even when the nuclear fluorescence was partially disturbed but still much stronger than that in the cytoplasm, the ΔANT(172)M1, ΔANT(172)M2, and ΔANT(172)M3 mutants still did not enhance AR-dependent transactivation. These results indicate that the basic amino acids within this 27 aa sequence may play roles in both the nuclear translocation and the transactivation function of ANT-1.

To test the receptor specificity of the transactivation domain of ANT-1 contained in ΔANT(172), a plasmid expressing ΔANT(172) was transiently transfected into COS-7 cells with an expression plasmid for the AR, GR or ER α. As shown in Fig. 4, co-expression of ΔANT(172) specifically enhanced either the AR or GR, but not ER α, in a dose-dependent manner until the molar ratio of ANT-1:AR was 4:1. When the quantity of the ANT-1 expression plasmid was extremely high (10:1), the TK-driven promoter harboring the estrogen response element or the TK promoter itself was enhanced by twofold. Under these experimental conditions, the AR- or GR-dependent transactivation system was enhanced by 12- to 15-fold. Overall, these results suggest that ΔANT(172) primarily represents the receptor specificity of ANT-1.

ANT-1 binds to AR-AF-1 through TPR motifs

We first performed mammalian two-hybrid assays using AR-AF-1 and ANT-1 deletion mutants. Possibly because

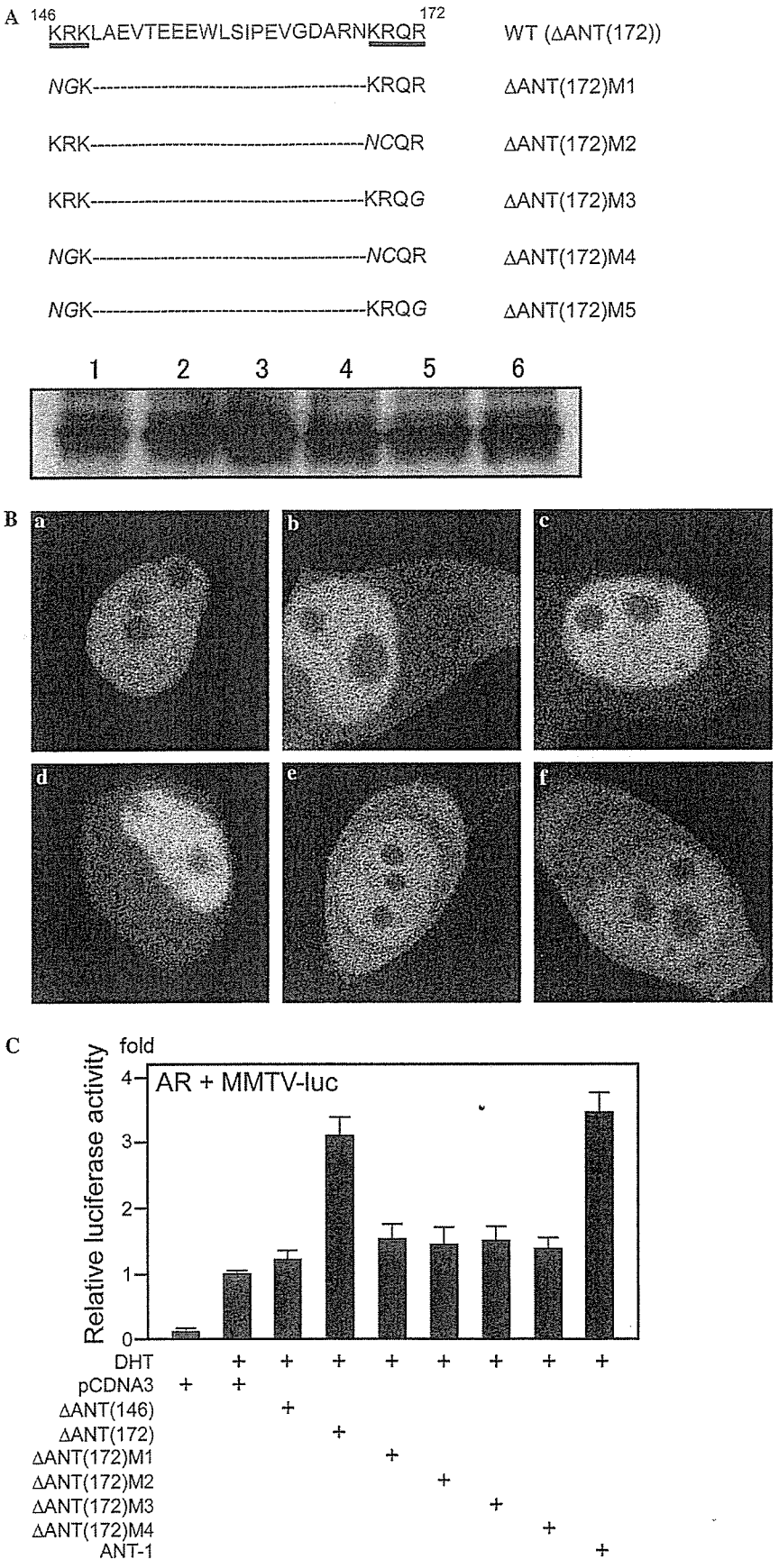
A
146
KRKLAEVTEEEWLSIPEVGDARNKRQR
172
WT (ΔANT(172))
NGK----------KRQR
ΔANT(172)M1
KRK----------NCQR
ΔANT(172)M2
KRK----------KRQG
ΔANT(172)M3
NGK----------NCQR
ΔANT(172)M4
NGK----------KRQG
ΔANT(172)M5
1 2 3 4 5 6
B
a
b
c
d
e
f
C
fold
Relative luciferase activity
AR + MMTV-luc
0
1
2
3
4
DHT + + + + + + + + +
pCDNA3 + +
ΔANT(146) +
ΔANT(172) +
ΔANT(172)M1 +
ΔANT(172)M2 +
ΔANT(172)M3 +
ΔANT(172)M4 +
ANT-1 +

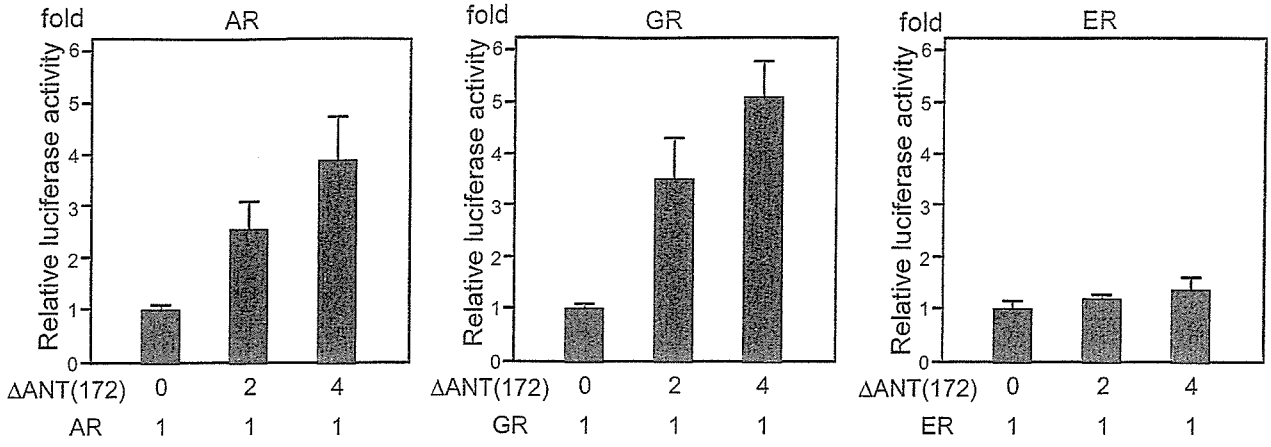

Fig. 4. Receptor-specific transactivation of ΔANT(172). An expression plasmid for ΔANT(172) was transiently transfected into COS-7 cells with expression plasmids for the AR, GR or ER α, together with appropriate reporter plasmids (pMMTV-luc for the AR or GR, and pERE2-tk109-luc for ER α), and then treated with steroid hormones (10^{-8} M DHT, 10^{-7} M dexamethasone or 10^{-8} M estradiol). Co-transfection of the plasmid expressing ΔANT(172) shows specific enhancement of the AR and GR, but not ER α, in a dose-dependent manner until the molar ratio of ANT-1 to the AR or GR reaches 4:1.

AR-AF-1 possesses strong autonomous transactivation capacity, transfection of NIH3T3 cells with the empty VP16 plasmid without any insertion conferred background luciferase activity driven by the GAL-4-containing AR-AF-1 (ΔAR(660)). Therefore, the background activity exerted by the presence of GAL-ΔAR(660) and the VP16 plasmid without an insertion was set as the standard and compared to the activities induced with the VP16 plasmids containing the ANT-1 deletion mutants (Fig. 5). Insertion of full-length ANT-1 into the VP16 plasmid (VP-ANT) or ΔANT(499) truncated in the seventh TPR of the 19 TPR repeats (Fig. 1A) strongly increased the luciferase activities by fivefold. When the sequence from aa 399 (in the fourth TPR) to 499 was deleted, the luciferase activity was weakly increased by twofold. The VP16 plasmid harboring ANT-C, containing 12.5 TPR motifs located at the C-terminal side, also showed about a 2.5-fold increase in the luciferase activity.

Next, we performed immunoprecipitation experiments using lysates of COS-7 cells stably expressing AR-AF-1 (COS-AR-AF-1 cells) transfected with plasmids expressing the ANT-1 deletion mutants tagged with myc. As shown in Fig. 6, only full-length ANT-1 and ΔANT(499) were co-immunoprecipitated with AR-AF-1 (lanes 1 and 2), whereas the other deletion mutants, including ΔANT(399) and ANT-C, were not. Taken together, these results indicate that ANT-1 binds to AR-AF-1 primarily via aa 399–499, encompassing the region from the fourth to the seventh TPR motifs.

ANT-1 binds to the AR sequence between either aa 180–360 or aa 360–532 within AF-1

We created plasmids expressing the AR-AF-1 region divided into three smaller fragments, namely aa 1–180, aa 180–360, and aa 360–532, and performed mammalian two-hybrid assays using ΔAR(660) containing the whole NTD and the DNA-binding domain (DBD) as a control (Fig. 7A). The results revealed that both ΔAR(180–360) and ΔAR(360–532) bound to ΔANT(499), whereas ΔAR(180) did not. Furthermore, the binding was confirmed by immunoprecipitation experiments (Fig. 8). ΔANT(499) was co-immunoprecipitated with either ΔAR(180–360) or ΔAR(360–532) tagged with GAL.

Discussion

We have identified four distinct functional domains in the ANT-1 molecule, which enhances AR-AF-1 transactivation capacity. The four regions were: (1) an NLS

Fig. 3. The nuclear localization signal of ANT-1. (A) Wild-type (WT) and mutant (M1–M5) aa sequences generated by site-directed mutagenesis of ΔANT(172) for expression in COS-7 cells by transient transfection of expression plasmids. Only aa 146–172 are shown. In the WT sequence, the bipartite basic amino acid stretches are underlined. In the sequences of M1–M5, the mutated residue(s) are shown in italics. The lower panel shows the expressions of GFP fusion proteins of WT ΔANT(172) and its mutants in COS-7 cells. Western blot was performed using anti-GFP antibody. Lane 1, WT ΔANT(172); lane 2, ΔANT(172)M1; lane 3, ΔANT(172)M2; lane 4, ΔANT(172)M3; lane 5, ΔANT(172)M4; lane 6, ΔANT(172)M5. (B) Confocal microscopic images of GFP fusion proteins of WT ΔANT(172) and its mutants. COS-7 cells were transiently transfected with plasmids expressing the WT and mutant ΔANT(172)-GFP fusion proteins and then observed by confocal microscopy. (a) WT ΔANT(172); (b) ΔANT(172)M1; (c) ΔANT(172)M2; (d) ΔANT(172)M3; (e) ΔANT(172)M4; (f) ΔANT(172)M5. Mutants M1, M2, and M3 show partial disruption of the nuclear GFP fluorescence, while mutants M4 and M5 show almost complete disruption. (C) Transactivation capacities of WT and mutated ΔANT(172). The cDNA fragments expressing the mutated ΔANT(172)-GFP fusion proteins (M1–M5) were subcloned into pcDNA3 to create expression plasmids for this experiment. COS-7 cells were transfected with the empty pcDNA3 plasmid (pcDNA3) or pcDNA3 expressing the WT or mutated ΔANT(172), or WT ΔANT(146) as a control, together with a plasmid expressing the full-length AR (molar ratio 5:1) and a pMMTV-luc reporter plasmid, and then treated with 10^{-8} M DHT. The relative enhancement of the luciferase activity compared with that after co-transfection with the empty pcDNA3 plasmid in the presence of 10^{-8} M DHT is expressed as the -fold induction.

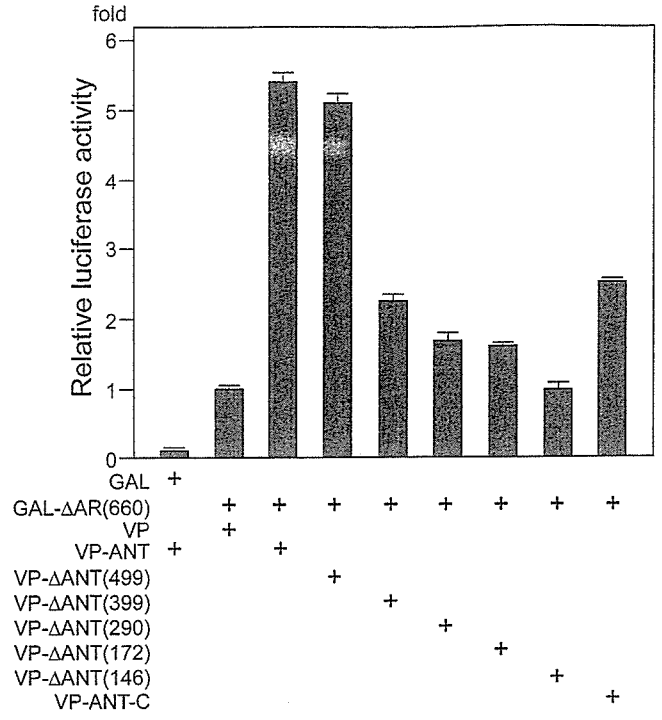

Fig. 5. Mammalian two-hybrid analysis to determine the domain within ANT-1 that binds to AR-AF-1. NIH3T3 cells were transiently transfected with 500 ng of pG5luc, 100 ng of VP16 plasmids containing full-length ANT-1 (VP-ANT) or ANT-1 truncated sequences (see Fig. 1A), and 300 ng of a GAL4 plasmid expressing aa 1–660 of the AR (see Fig. 7A) fused to GAL4. The background activity exerted by the presence of GAL-ΔAR(660) and the VP16 plasmid without an insertion was set as the standard for comparisons with the activities obtained with the VP16 plasmids containing the ANT-1 deletion mutants, and the data are presented as relative activities.

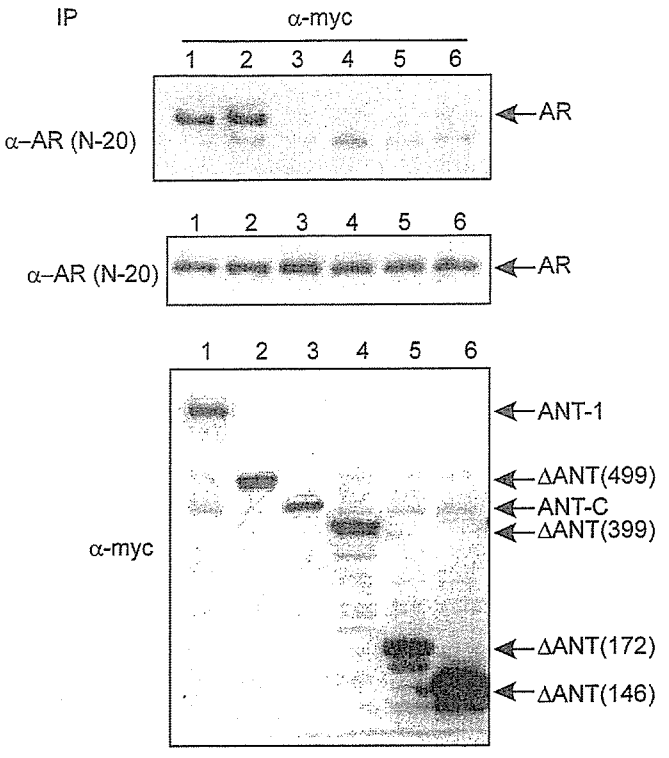

Fig. 6. Immunocoprecipitation of truncated ANT-1 mutants with AR-AF-1. COS-7 cells stably expressing AR-AF-1 (COS-7-AR-AF-1 cells) were transfected with plasmids expressing full-length or truncated mutants of ANT-1 tagged with myc. Immunoprecipitation (IP) was performed using an anti-myc antibody, and the precipitates were analyzed by Western blotting using an antibody against N-20 in AR-AF-1. The middle and bottom panels show the findings for the whole lysates used for the IP as controls. Lanes 1, full-length ANT-1; lanes 2, ΔANT(499); lanes 3, ANT-C; lanes 4, ΔANT(399); lanes 5, ΔANT(172); lanes 6, ΔANT(146).

domain; (2) a receptor-specific AF-1 transactivating domain; (3) an AR-AF-1-binding domain; (4) an intranuclear speckle formation domain. Both the NLS and ANT-1 transactivation domains were within the first 172 aa of the N-terminal region. Furthermore, the NLS of ANT-1 was tightly related to or closely overlapped with the sequence required for the transactivation function of ANT-1. Mutational analysis of the ANT-1 NLS revealed that the transactivation capacities of the intranuclear ANT-1 mutants were almost completely abolished after partial disruption of the nuclear translocation by mutations in either the first or second basic amino acid clusters. Another example of a tight relationship between a bipartite NLS and a transactivation function has been reported for the murine transcription factor distal-less (Dlx) 3, which is involved in the development and differentiation of epithelial tissue [31]. In the Dlx3 protein, the NLS sequences are part of the homeodomain sequence, and thus mutation of the NLS disrupts the sequence required for specific DNA binding, the transactivation potential, and protein–protein interactions [32]. The mechanisms for how the ANT-1 NLS confers the transactivation capacity still remain to be elucidated.

In contrast, the other two domains, required for either binding to AR-AF-1 or intranuclear speckle formation, were present within the first 7 of the 19 TPR motifs found in the ANT-1 molecule. The TPR is a structural motif present in a wide range of proteins and mediates protein–protein interactions for the assembly of multiprotein complexes. The TPR was first identified in 1990, and its name denotes the 34 amino acids comprising the basic repeat [24]. These basic repeats are usually arrayed in a tandem fashion. To date, the TPR motif has been identified in more than 25 proteins, which play important roles in diverse biological functions, including gene transcription and pre-mRNA splicing. The TPR motif has been shown to possess biological significance, since congenital mutations within the motif result in congenital disorders, such as Leber congenital amaurosis [33] and chronic granulomatous disease [34].

ANT-1 is identical to the mammalian nucleoprotein PRP6, which binds to the human splicing factor U5 snRNP (GenBank Accession No. AF221842). During the splicing step, snRNPs play critical roles in constructing the multiprotein–RNA complex known as the spliceosome. The splicing snRNPs (U1, U2, U4/U6, and U5) associate with the pre-mRNA and then with each other in an ordered

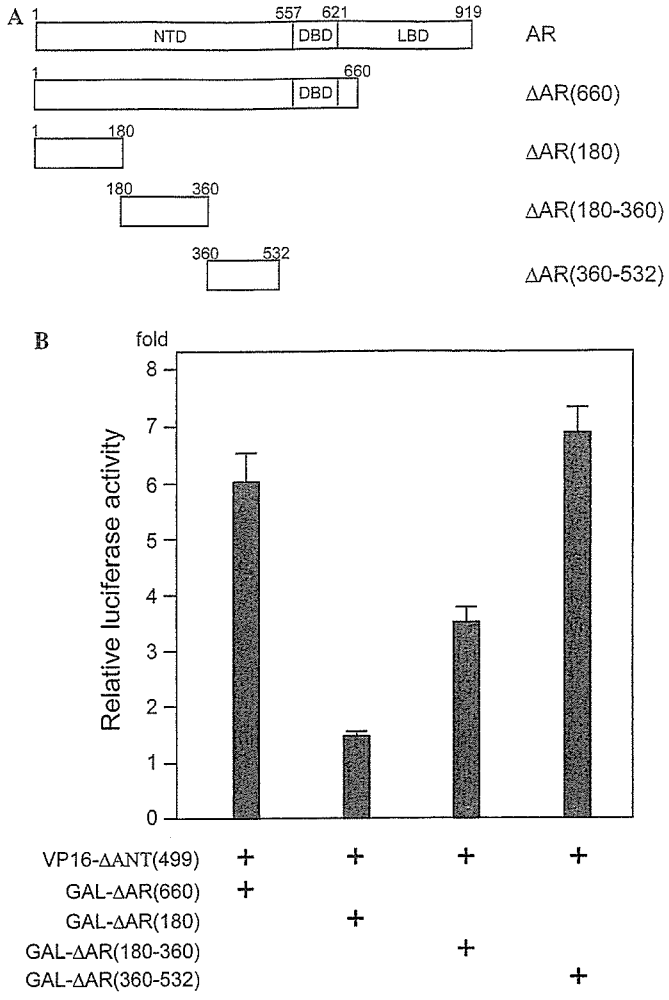

Fig. 7. Mammalian two-hybrid analysis to determine the domain within AR-AF-1 that binds to ANT-1. (A) Schematic diagrams of the truncated mutants of AR-AF-1 used for the experiment. NTD, N-terminal domain; DBD, DNA-binding domain; LBD, ligand-binding domain. (B) Mammalian two-hybrid analysis. NIH3T3 cells were transiently transfected using 500 ng of pG5luc, 100 ng of the VP16 plasmid containing ΔANT(499), or the VP16 plasmid without an insertion as a control, and 300 ng of GAL4 plasmids expressing fusion proteins with truncated mutants of the AR. In each transfection, the background activity exerted by the presence of GAL-ΔARs and the VP16 plasmid without an insertion was set as the standard for comparisons with the activities obtained with the VP16 plasmid containing ΔANT(499), and the data are expressed as the relative activities.

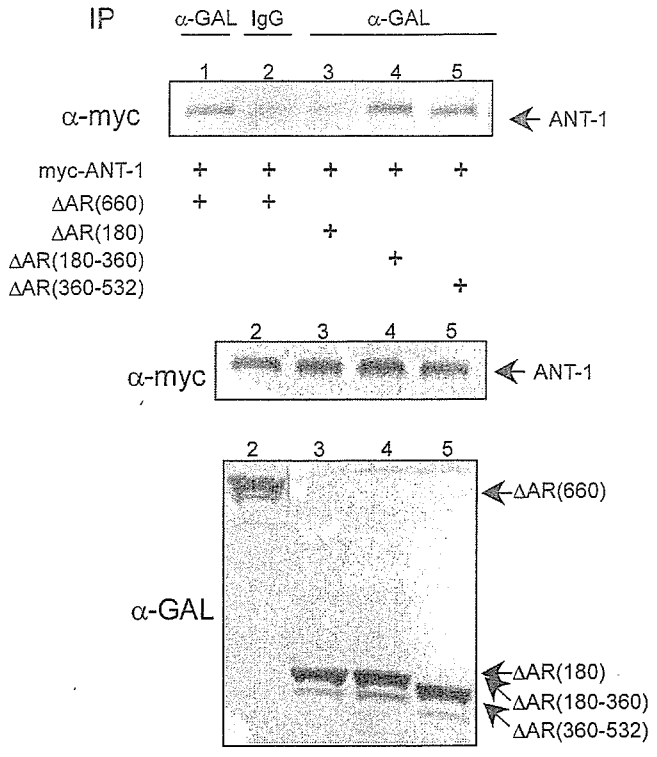

Fig. 8. Immunocoprecipitation of truncated AR mutants with ANT-1. COS-7 cells were transiently transfected with plasmids expressing truncated mutants of the AR tagged with GAL and ΔANT(499) tagged with myc. Immunoprecipitation (IP) was performed using an anti-GAL antibody for lanes 1, 3, 4, and 5 and non-immune IgG (*IgG*) for lane 2 as a control, and the precipitates were analyzed by Western blotting using an anti-myc antibody for ΔANT(499). The middle and bottom panels show the findings for the whole lysates used for the IP as controls. Lanes 1 and 2, ΔAR(660); lanes 3, ΔAR(180); lanes 4, ΔAR(180–360); lanes 5, ΔAR(360–532).

sequence to form the spliceosome, during which U5 snRNA base-pairs with exon sequences flanking the split sites. Through the sequence from aa 290 to 399 at the N-terminal end of the long TPR domain, ANT-1 may bind to the U5 snRNP multiprotein complex in the SFC, thereby forming subnuclear speckles. Although prp6p, a yeast homolog of ANT-1, was originally isolated as a spliceosomal protein, we did not observe any ANT-1-mediated enhancement of the splicing efficiency when assessed using an artificial minigene [19]. Therefore, we previously speculated that ANT-1 per se did not possess any splicing activity, but instead functioned as a transcriptional coactivator. This is in strong contrast to a spliceosomal protein SF3a p120 which is the coactivator specific for ER α-AF1 through the modulation of RNA splicing efficiency via ER α Ser118 phosphorylation [35]. In this regard, ΔANT(172), which may be unable to bind to U5 snRNP due to the absence of all the TPR motifs, showed enhancement of the AR- or GR-dependent transactivation function, but not of ER-dependent transactivation. These findings also indicated that the receptor specificity of the ANT-1-dependent transactivation function was determined by dual mechanisms: (1) via the binding specificity of ANT-1 to cognate receptors such as the AR or GR mediated by the direct binding using TPR motifs; (2) via the receptor-specific enhancement of the transactivation capacity caused by residues between aa 1 and 172, among which aa 146–172 were sufficient for the transactivation function per se. The latter receptor specificity apparently did not require the direct binding to the AR-AF-1, thus it may be exerted by another putative coactivator(s) or enhancer(s) with specific functions.

In good agreement with the subnuclear distribution of prp6p (a yeast homolog of ANT-1) [36], the intranuclear ANT-1 distribution was identical to the known distribution patterns of splicing factors [37]. Transfected ANT-1

showed two distinct distributions in the nucleus as follows: a diffuse fine reticular distribution throughout the nucleus, except for the nucleolus, and a coarsely clustered distribution (speckles) known as the SFC. In a previous paper, we speculated that the subnuclear speckle formation by ANT-1 could be independent of its transactivation function, and thus the merging of the diffuse ANT-1 distribution with the AR speckles may represent the area where ANT-1 or the ANT-1–snRNP complex meets the active AR–cofactor complex [19]. This hypothesis was supported by the current observation that the ANT-1 deletion mutants that were unable to form speckles in the nucleus retained almost the full transactivation capacity for AR-AF-1 (Figs. 1 and 2). Interestingly, mammalian PRP4K kinase (PRP4K) has been shown to be a U5 snRNP-associated kinase that interacts with BRG1, N-CoR, and mammalian PRP6 (ANT-1), and possibly phosphorylates BRG1 and PRP6 [38]. Taken together with our findings, U5 snRNP may play a role in transcription-splicing coupling.

ANT-1 bound to aa 180–360 and 360–532, respectively, within AR-AF-1. Previous studies have assigned AR-AF-1 (also called the transactivation domain or TAD) to aa 142–485 of the receptor. This region comprises both the transcription activation unit (TAU)-1 (aa 101–360) and TAU-5 (aa 360–485) domains [39,40], both of which clearly overlap with the two regions required for binding to ANT-1. Recent studies have revealed that AR-AF-1 lacks a stable secondary structure in aqueous solution, and instead is a structurally flexible polypeptide that folds into a more compact conformation in the presence of structure-stabilizing solutes [41,42]. Hence, the folding of AR-AF-1 in response to specific protein–protein interactions may create a platform for subsequent interactions in the fully competent transactivation complex. This may explain why AR-AF-1 binds many unique proteins, including a subunit of the TFIIF general transcription factor and snRNPs. In this regard, the multiple TPRs present in ANT-1 may play a role in further providing a platform for such interactions.

Acknowledgments

This study was partly supported by Grants-in-Aid for Scientific Research from the Ministry of Education, Culture, Sports, Science and Technology (to K.G. and H.N., respectively) and partly by Core Research for Evolutional Science and Technology from the Japan Science and Technology Agency (to H.N. from 1999 to 2003).

References

[1] M. Beato, S. Chavez, M. Truss, Transcriptional regulation by steroid hormones, Steroids 61 (1996) 240–251.

[2] C.L. Bevan, S. Hoare, F. Claessens, D.M. Heery, M.G. Parker, The AF1 and AF2 domains of the androgen receptor interact with distinct regions of SRC1, Mol. Cell. Biol. 19 (1999) 8383–8392.

[3] P. Alen, F. Claessens, G. Verhoeven, W. Rombauts, B. Peeters, The androgen receptor amino-terminal domain plays a key role in p160 coactivator-stimulated gene transcription, Mol. Cell. Biol. 19 (1999) 6085–6097.

[4] L. Tora, J. White, C. Brou, D. Tasset, N. Webster, E. Scheer, P. Chambon, The human estrogen receptor has two independent nonacidic transcriptional activation functions, Cell 59 (1989) 477–487.

[5] C.A. Quigley, A. De Bellis, K.B. Marschke, M.K. el-Awady, E.M. Wilson, F.S. French, Androgen receptor defects: historical, clinical, and molecular perspectives, Endocr. Rev. 16 (1995) 271–321.

[6] L. Tora, H. Gronemeyer, B. Turcotte, M.P. Gaub, P. Chambon, The N-terminal region of the chicken progesterone receptor specifies target gene activation, Nature 333 (1988) 185–188.

[7] M. Adachi, R. Takayanagi, A. Tomura, K. Imasaki, S. Kato, K. Goto, T. Yanase, S. Ikuyama, H. Nawata, Androgen-insensitivity syndrome as a possible coactivator disease, N. Engl. J. Med. 343 (2000) 856–862.

[8] V.V. Ogryzko, R.L. Schiltz, V. Russanova, B.H. Howard, Y. Nakatani, The transcriptional coactivators p300 and CBP are histone acetyltransferases, Cell 87 (1996) 953–959.

[9] M.L. Lu, M.C. Schneider, Y. Zheng, X. Zhang, J.P. Richie, Caveolin-1 interacts with androgen receptor. A positive modulator of androgen receptor mediated transactivation, J. Biol. Chem. 276 (2001) 13442–13451.

[10] J. Reid, I. Murray, K. Watt, R. Betney, I.J. McEwan, The androgen receptor interacts with multiple regions of the large subunit of general transcription factor TFIIF, J. Biol. Chem. 277 (2002) 41247–41253, Epub 42002 Aug 41213.

[11] X. Yu, P. Li, R.G. Roeder, Z. Wang, Inhibition of androgen receptor-mediated transcription by amino-terminal enhancer of split, Mol. Cell. Biol. 21 (2001) 4614–4625.

[12] S.A. Hayes, M. Zarnegar, M. Sharma, F. Yang, D.M. Peehl, P. ten Dijke, Z. Sun, SMAD3 represses androgen receptor-mediated transcription, Cancer Res. 61 (2001) 2112–2118.

[13] H. Dotzlaw, U. Moehren, S. Mink, A.C. Cato, J.A. Iniguez Lluhi, A. Baniahmad, The amino terminus of the human AR is target for corepressor action and antihormone agonism, Mol. Endocrinol. 16 (2002) 661–673.

[14] P.W. Hsiao, C. Chang, Isolation and characterization of ARA160 as the first androgen receptor N-terminal-associated coactivator in human prostate cells, J. Biol. Chem. 274 (1999) 22373–22379.

[15] S.M. Markus, S.S. Taneja, S.K. Logan, W. Li, S. Ha, A.B. Hittelman, I. Rogatsky, M.J. Garabedian, Identification and characterization of ART-27, a novel coactivator for the androgen receptor N terminus, Mol. Biol. Cell 13 (2002) 670–682.

[16] A. Yamamoto, Y. Hashimoto, K. Kohri, E. Ogata, S. Kato, K. Ikeda, M. Nakanishi, Cyclin E as a coactivator of the androgen receptor, J. Cell Biol. 150 (2000) 873–880.

[17] J.J. Park, R.A. Irvine, G. Buchanan, S.S. Koh, J.M. Park, W.D. Tilley, M.R. Stallcup, M.F. Press, G.A. Coetzee, Breast cancer susceptibility gene 1 (BRCA1) is a coactivator of the androgen receptor, Cancer Res. 60 (2000) 5946–5949.

[18] R.B. Lanz, N.J. McKenna, S.A. Onate, U. Albrecht, J. Wong, S.Y. Tsai, M.J. Tsai, B.W. O'Malley, A steroid receptor coactivator, SRA, functions as an RNA and is present in an SRC-1 complex, Cell 97 (1999) 17–27.

[19] Y. Zhao, K. Goto, M. Saitoh, T. Yanase, M. Nomura, T. Okabe, R. Takayanagi, H. Nawata, Activation function-1 domain of androgen receptor contributes to the interaction between subnuclear splicing factor compartment and nuclear receptor compartment. Identification of the p102 U5 small nuclear ribonucleoprotein particle-binding protein as a coactivator for the receptor, J. Biol. Chem. 277 (2002) 30031–30039, Epub 32002 May 30030.

[20] A. Nishikimi, J. Mukai, N. Kioka, M. Yamada, A novel mammalian nuclear protein similar to *Schizosaccharomyces pombe* Prp1p/Zer1p and *Saccharomyces cerevisiae* Prp6p pre-mRNA splicing factors, Biochim. Biophys. Acta 1435 (1999) 147–152.